Scientia Iranica B (2018) 25(2), 675–688

Sharif University of Technology
Scientia Iranica
Transactions B: Mechanical Engineering
http://scientiairanica.sharif.edu

Bending and vibration analysis of delaminated Bernoulli-Euler microbeams using the modified couple stress

R.-A. Jafari-Talookolaei[a,*], N. Ebrahimzade[a], S. Rashidi-Juybari[a], and K. Teimoori[b]

a. *Department of Mechanical Engineering, Babol Noshirvani University of Technology, Babol, P.O. Box 47148-71167, Iran.*
b. *Department of Mechanical Engineering, The City College of the City University of New York, NY 10031, USA.*

Received 25 September 2015; received in revised form 6 December 2016; accepted 25 February 2017

KEYWORDS
Delaminated microbeam;
Free vibration;
Modified couple stress theory;
Free and constrained models.

Abstract. In this paper, we study static bending and free vibration behaviors of Bernoulli-Euler microbeams with a single delamination using the modified couple stress theory. The delaminated beam is modeled by four interconnected sub-beams using the delamination zone as their boundaries. The free and constrained mode theories are utilized to model the interaction of delamination surfaces in the damaged area. The continuity as well as compatibility conditions are satisfied between the neighboring sub-beams. After verification of the results for some case studies with available solutions, the effects of various parameters, such as spanwise and thicknesswise locations of the delamination, material length-scale parameter, and boundary conditions, on the static bending and free vibration characteristics of the size-dependent microbeam, have been investigated in detail.

1. Introduction

Microstructure-dependent structural components and their mechanical behavior have attracted considerable research efforts among scholars in recent years. This is due to the wide application of small-scale systems to various engineering disciplines where miniaturized substructures, such as microbeams, micro-plates, and/or microbars, are their key building blocks. In particular, when the overall spatial resolution of system is comparable to the size of the material length-scale parameter in its subcomponents (e.g., characteristic size of crystal lattices, molecules of polymers, and particles of granular materials), the well-known classical theories are inadequate to capture the size dependency of these substructures; thus, they no longer present an accurate mathematical framework to study the real physics of the whole model. Therefore, several higher order (nonlocal) theories, such as micro polar, strain gradient, couple stress, as well as modified couple stress theories, have been proposed for isotropic elastic materials in which the role(s) of material length-scale parameter/s is/are involved in the constitutive equations.

Beam-like members are important elements that are extensively used in the small-scale systems, and the size-dependent study of their dynamic properties has widespread applications. Thus, due to the rapid development of small-scale technologies in recent years, many studies have been carried out to investigate the behavior of microbeams (e.g., the application of microbeams in micro actuators [1], biosensors [2], atomic

*. *Corresponding author. Tel.: +98 11 32332071-4 (Int. 1453); Fax: +98 11 32339214*
E-mail addresses: ra.jafari@nit.ac.ir (R.-A. Jafari-Talookolaei); N.Ebrahimzade2@newcastle.ac.uk (N. Ebrahimzade); srj_mechanics@yahoo.com. (S. Rashidi-Juybari); Teimoori@me.ccny.cuny.edu (K. Teimoori)

doi: 10.24200/sci.2017.4252

force microscopes [3], and carrying micro-particles [4]). In this regard, the couple stress elasticity theory was presented in 1960s for the first time where this model introduced two higher-order material length-scale parameters, in addition to the two classical Lamé constants, in the governing equations of motion [5,6]. In 2002, this model was modified by Yang et al. [7] to develop the modified couple stress theory in which the constitutive equations contain only one additional material length scale, creating symmetric couple stress tensor. These two properties of the modified couple stress theory (i.e., the inclusion of a symmetric couple stress tensor and the involvement of only one length-scale parameter) are two advantages of this model over the classical couple stress theory. Therefore, in the past decade, many researchers have studied the behavior of microbeams based on this novel and convenient theory. For instance, modified couple stress theory for bending analysis of Bernoulli-Euler beams was presented using the minimum total potential energy principle [8]. Ma et al. [9] developed size-dependent Timoshenko beam model based on the modified couple stress theory. They also investigated the Poisson's effect on the static bending and free vibration of a simply supported beam. However, later, it was shown that considering Poisson's effect can lead to erroneous results, and the results obtained by omitting Poisson's effect are much closer to the experimental data [10,11]. Kahrobaiyan et al. [12] used modified couple stress theory to obtain the dynamic characteristics of atomic force microscopes cantilevers. Asghari et al. investigated the static and free vibration analyses of nonlinear Timoshenko beam based on the modified couple stress theory [13]. Akgöz and Civalek reported on the stability of axially loaded microbeams based on the strain gradient elasticity and modified couple stress theory [14]. Simsek and Reddy [15] examined the static and dynamic behaviors of the functionally graded microbeams based on the modified couple stress theory, compared with other nonlocal beam theories. Akgöz et al. studied the vibration responses of non-homogenous and non-uniform microbeams within the framework of Bernoulli-Euler beam model and modified couple stress theory [16]. In addition, Mohammad Abadi and Daneshmehr investigated the buckling analyses of laminated composite beams based on the Bernoulli-Euler and Timoshenko beam theories by the modified couple stress theory [17]. Darijani and Mohammadabadi proposed a new beam deformation theory using the modified couple stress theory by considering the shear deformation with two unknown functions [18].

Similar to the aforementioned linear models, the nonlinear static and dynamic analyses of microbeams were investigated using the numerical and theoretical methods by many researchers based on the modified couple stress theory [19-23]. Dai et al. developed a new nonlinear theoretical model for cantilever microbeams [19] to explore the nonlinear dynamic behavior. Mohammad-Abadi and Daneshmehr [20] reported on the buckling analysis of microbeams based on the Bernoulli-Euler beam, Timoshenko beam, and Reddy beam theories. By employing the principle of minimum total potential energy, they derived the governing differential equations and corresponding boundary conditions. Generalized differential quadrature method was employed to solve the governing differential equations. Simsek [21] used the modified couple stress theory to study the static and nonlinear vibration analyses of microbeams rested on a three-layered nonlinear elastic foundation. The Bernoulli-Euler beam theory along with the von-Kármán's geometric nonlinearity was used in this study. Ghayesh et al. numerically studied the nonlinear resonant dynamics of a microbeam [22] for straight beam, and Farokhi et al. [23] did the same for an initially curved beam. The Galerkin method along with appropriate eigenfunctions was used to discretize the nonlinear partial differential equation of motion into a set of nonlinear ordinary differential equations, and subsequently, the pseudo-arc length continuation technique was utilized to solve these equations.

On the other hand, it is well known that the beam-like elements may encounter different types of damages during their manufacturing process or service life. Among them, delamination (or through-the-width crack) is found to be a common failure mode in beams where it is well known that the incidence of the delamination in a structure changes its dynamic characteristics such as natural frequencies and dynamic response. Accordingly, there has been a growing interest in studying the vibrational behavior of delaminated beams. Wang et al. [24] investigated the free vibrations of an isotropic beam with a through-the-width delamination by splitting the whole beam into four intact Bernoulli-Euler beams called sub-beams that are joined together. In their study, the delaminated layers were assumed to deform 'freely' without any interaction over the delamination surfaces (*free mode model*); thus, they have different transverse deformations. According to this modeling, the dramatic interpenetration of the sub-beams located in the delaminated region may occur in the case of off mid-plane delamination, which is physically impossible. To avoid this kind of inconsistency, a new model was presented by Mujumdar and Suryanarayan [25], which is based on the assumption that the delaminated layers are constrained to have the same transverse deformations (*constrained mode model*). However, this constrained model cannot predict the opening in the mode shapes found in the experiments by Shen and Grady [26]. Afterwards, many researchers have used the free and constrained models to study the dynamics of delaminated beams. For instance, Della et al. presented an analytical solution

to the free vibrations of a beam with two overlapped delaminations [27]. The fundamental frequency and linear normal mode of the beam, influenced by the size and location of delamination, were investigated in their study. Manoach and Warminski [28] presented dynamic behavior of a composite Timoshenko beam with a single delamination. Kargarnovin et al. studied on the transient response of a delaminated composite Timoshenko beam under the action of moving loads and moving oscillating masses [29,30]. In these studies, the contact interactions between the delaminated surfaces were modeled using the constrained mode model [29] and piecewise linear contact springs [30] (the contact springs were used to investigate two extreme cases, i.e. free and constrained models). The effects of different parameters, such as the size and depth of the delamination, the load velocity, the different ply configurations, and the Poisson's effect on the dynamic response of the beam, were studied. Moreover, Szekrényes investigated the free vibration analysis of delaminated composite beams based on the Timoshenko and Bernoulli-Euler beam theories [31]. In this study, it was shown that the delaminated beam vibration is a coupled flexural-longitudinal vibration, and the delamination opening is due to the dynamic buckling phenomenon. Furthermore, Szekrényes [32] also presented a finite-element model for delaminated composite beams to investigate the existence of a system response to the parametric excitation, and bifurcation, and stability analysis of the possible solution. Recently, Attar et al. [33,34] have studied non-smooth static and dynamic behaviors of structural components interacting with the unilateral elastic foundations. They proposed a shooting technique to obtain the non-linear normal modes of beams interacting with the tensionless elastic supports. In these studies, the damaged (non-smooth) contact interactions at the interface of beam and foundation can be interpreted as the delamination damage compared to the corresponding system with a perfect bilateral connection between the beam and elastic supports at their interface.

Although there are numerous publications on the dynamic behavior of damaged classical structures or the role of size dependency in the dynamics of intact microbeams, we can observe from the literature survey that there is no contribution to the static and dynamic analyses of delaminated microbeams. Hence, the main contribution of the present work is to analyze the bending and vibration characteristics of a Bernoulli-Euler microbeam with a single delamination. In this study, we utilize both free and constrained mode theories to model the delaminated surfaces. Subsequently, some numerical examples are presented to investigate the effects of different delamination parameters, such as the damage length, size, and thicknesswise location, on the static and dynamic behaviors of the system.

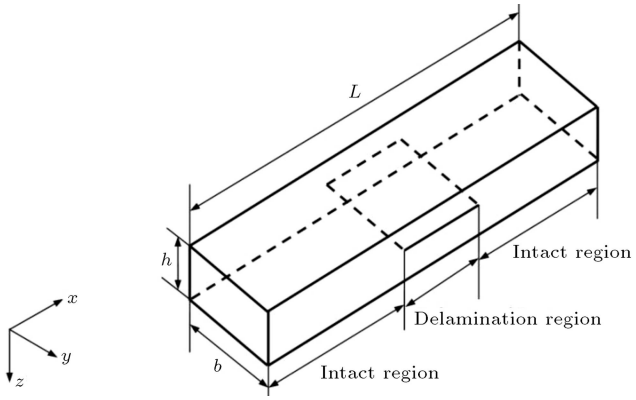

Figure 1. The schematic model of a delaminated microbeam.

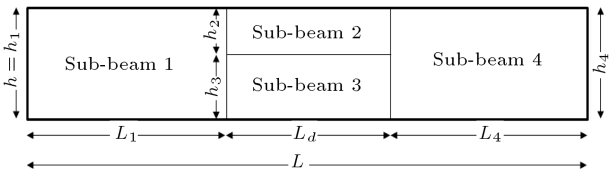

Figure 2. Representation of a delaminated microbeam with four sub-beams.

2. Assumptions

The considered microbeam with length L has a rectangular cross-section of height h and width b, as depicted in Figure 1. There is an embedded delamination of length L_d located at a distance L_1 from the left end and a depth of h_2 with respect to the upper edge. The delaminated beam can be modeled as a combination of four sub-beams connected at delamination boundaries, i.e. $x = L_1$ and $x = L_1 + L_d$, as demonstrated in Figure 2. Thus, we have four sub-beams numbered from 1 to 4 with the lengths of L_i and thicknesses of h_i, where $i = 1 \cdots 4$, $L_2 = L_3 = L_d$, $h_1 = h_4 = h$, and $L_4 = L - (L_1 + L_d)$.

3. Formulations

3.1. Preliminaries

The modified couple stress theory that was proposed in [7] is used in this study. In fact, this theory is an extension of the classical couple stress theory. Accordingly, the strain energy, U, of an isotropic linear elastic material with the total volume of Ω can be expressed as follows:

$$U = \frac{1}{2} \iiint_{\Omega} (\sigma : \varepsilon + m : \chi) dv, \tag{1}$$

where dv is the differential volume element, σ is the Cauchy stress tensor, ε is the strain tensor, m is the deviatoric part of the couple stress tensor, and χ is the symmetric curvature tensor. These parameters are defined as follows:

$$\varepsilon = \frac{1}{2}\left[\nabla u + (\nabla u)^T\right], \tag{2}$$

$$\sigma = \lambda tr(\varepsilon) I + 2\mu\varepsilon, \tag{3}$$

$$\chi = \frac{1}{2}\left[\nabla\theta + (\nabla\theta)^T\right], \tag{4}$$

$$m = 2\ell^2\mu\chi, \tag{5}$$

where θ is the rotation vector defined by Eq. (6) as follows:

$$\theta = \frac{1}{2} curl(u), \tag{6}$$

where u is the displacement vector, ℓ is the material length scale, and λ and μ are the Lamé's constants so that they are related to both Young's modulus, E, and Poisson's ratio, v, as follows:

$$\lambda = \frac{Ev}{(1+v)(1-2v)}, \tag{7}$$

$$\mu = \frac{E}{2(1+v)}. \tag{8}$$

3.2. Governing equations

According to the Bernoulli-Euler beam theory, the displacement field for the ith sub-beam can be expressed as follows:

$$u_i = -z\frac{(\partial w_i(x,t)}{\partial x}, \qquad v_i = 0,$$
$$w_i = w_i(x,t), \qquad i = 1, \cdots, 4, \tag{9}$$

where u_i, v_i, and w_i are the components of displacement vector in the directions of x, y, and z, respectively. By substituting Eq. (9) into Eq. (2), the strain components of the ith sub-beam can be obtained as follows:

$$\varepsilon_{xx_i} = -z\frac{\partial^2 w_i(x,t)}{\partial x^2},$$
$$\varepsilon_{yy_i} = \varepsilon_{zz_i} = \varepsilon_{xy_i} = \varepsilon_{yz_i} = \varepsilon_{zx_i} = 0. \tag{10}$$

Furthermore, using Eqs. (3)-(8), one can obtain the stress components, rotation vector, symmetric curvature tensor, and deviatoric part of the couple stress tensor as follows:

$$\sigma_{xx_i} = -(\lambda+2\mu)z\frac{\partial^2 w_i}{\partial x^2},$$
$$\sigma_{yy_i} = \sigma_{zz_i} = -\lambda z\frac{\partial^2 w_i}{\partial x^2},$$
$$\sigma_{xy_i} = \sigma_{yz_i} = \sigma_{zx_i} = 0, \tag{11}$$

$$\theta_i = \frac{1}{2}\begin{vmatrix} \hat{i} & \hat{J} & \hat{k} \\ \frac{\partial}{\partial x} & \frac{\partial}{\partial y} & \frac{\partial}{\partial z} \\ -z\frac{\partial w_i}{\partial x} & 0 & w_i \end{vmatrix} = \left(0, -\frac{\partial w_i}{\partial x}, 0\right), \tag{12}$$

$$\chi_i = \begin{vmatrix} 0 & -\frac{1}{2}\frac{\partial^2 w_i}{\partial x^2} & 0 \\ -\frac{1}{2}\frac{\partial^2 w_i}{\partial x^2} & 0 & 0 \\ 0 & 0 & 0 \end{vmatrix}, \tag{13}$$

$$m_i = \begin{vmatrix} 0 & -\ell^2\mu\frac{\partial^2 w_i}{\partial x^2} & 0 \\ -\ell^2\mu\frac{\partial^2 w_i}{\partial x^2} & 0 & 0 \\ 0 & 0 & 0 \end{vmatrix}. \tag{14}$$

By substituting Eqs. (10)-(14) into Eq. (1), the expression for strain energy of four sub-beams can be obtained as follows:

$$U_1 = \frac{1}{2}\int_0^{L_1}\left\{(\lambda+2\mu)I_1\left(\frac{\partial^2 w_1}{\partial x^2}\right)^2 + \mu\ell^2 A_1\left(\frac{\partial^2 w_1}{\partial x^2}\right)^2\right\}dx, \tag{15}$$

$$U_i = \frac{1}{2}\int_{L_1}^{L_1+L_d}\left\{(\lambda+2\mu)I_i\left(\frac{\partial^2 w_i}{\partial x^2}\right)^2 + \mu\ell^2 A_i\left(\frac{\partial^2 w_i}{\partial x^2}\right)^2\right\}dx, \qquad i = 2, 3, \tag{16}$$

$$U_4 = \frac{1}{2}\int_{L_1+L_d}^{L}\left\{(\lambda+2\mu)I_4\left(\frac{\partial^2 w_4}{\partial x^2}\right)^2 + \mu\ell^2 A_4\left(\frac{\partial^2 w_4}{\partial x^2}\right)^2\right\}dx, \tag{17}$$

where:

$$I_i = \iint_{A_i} z^2 dA, \qquad i = 1 \cdots 4, \tag{18}$$

and A_i is the cross-sectional area of the ith sub-beam. Furthermore, the kinetic energy of sub-beams can be expressed as follows:

$$T_1 = \frac{1}{2}\int_0^{L_1}\rho A_1\left(\frac{\partial w_1}{\partial t}\right)^2 dx, \tag{19}$$

$$T_i = \frac{1}{2}\int_{L_1}^{L_1+L_d}\rho A_i\left(\frac{\partial w_i}{\partial t}\right)^2 dx, \qquad i = 2, 3, \tag{20}$$

$$T_4 = \frac{1}{2}\int_{L_1+L_d}^{L}\rho A_4\left(\frac{\partial w_4}{\partial t}\right)^2 dx. \tag{21}$$

Finally, the work done by external forces and moments can be obtained as [8]:

$$W = \iint_{\Omega}(f.u + c.\theta)dv + \iint_{\partial\Omega}(t.u + s.\theta)da, \tag{22}$$

where f, c, t, and s are the body force, body couple, surface traction, and surface couple, respectively, and $\partial\Omega$ is the surface of Ω.

3.2.1. Static analysis

In this section, the static bending analysis of the delaminated microbeam is presented. The differential equations for each sub-beam are derived using the principle of minimum total potential energy, which can be expressed as [35]:

$$\delta\Pi = \delta(U - W) = 0, \tag{23}$$

where δ is the variational operator. Moreover, by definition, the total potential energy (Π) is written as follows:

$$\Pi = U - W = U_1 + U_2 + U_3 + U_4 - W. \tag{24}$$

The related equations according to both constrained and free modes are presented in the following subsections.

Constrained mode

According to constrained mode model [25], sub-beams located in the delamination region have identical transverse displacement, i.e. $w_2 = w_3$. Using Eq. (23), the governing equations for the static bending of sub-beams in this case are obtained as follows:

$$D_i \frac{d^4 w_i(x)}{dx^4} - q_i(x) = 0, \qquad i = 1, 4, \tag{25}$$

$$(D_2 + D_3)\frac{d^4 w_2(x)}{dx^4} - q_2(x) = 0, \tag{26}$$

where:

$$D_i = (\lambda + 2\mu) I_i + \mu \ell^2 A_i, \qquad i = 1 - 4. \tag{27}$$

In addition, q_i ($i = 1, 2$, and 4) is the external load applied to the ith sub-beams. The linear non-homogeneous differential Eqs. (25) and (26) can be integrated to obtain the following solutions:

$$w_i(x) = \frac{1}{D_i}\left(\iint\iint q_i(x)dxdxdxdx + \frac{C_{1i}}{6}x^3 + \frac{C_{2i}}{2}x^2 + C_{3i}x + C_{4i}\right), \qquad i = 1 \text{ and } 4, \tag{28}$$

$$w_2(x) = \frac{1}{D_2 + D_3}\left(\iint\iint q_2(x)dxdxdxdx + \frac{C_{12}}{6}x^3 + \frac{C_{22}}{2}x^2 + C_{32}x + C_{42}\right), \tag{29}$$

where coefficients C_{ji} are unknown constants that can be determined by applying appropriate boundary, continuity, and compatibility conditions (details are presented in Section 3.2.2). Note that Eqs. (28) and (29) represent the closed-form solution for the static deflection of the delaminated microbeam.

Free mode

In the free mode model, as mentioned before, sub-beams 2 and 3 were allowed to move freely without touching each other. Thus, they have different transverse displacements. By employing a similar process as used in the previous subsection, the governing equations of the sub-beams can be obtained as follows:

$$D_i \frac{d^4 w_i(x)}{dx^4} - q_i(x) = 0, \qquad i = 1, \cdots, 4. \tag{30}$$

By integrating Eq. (30), the static deflection of the delaminated microbeam will be obtained by the following formula:

$$w_i(x) = \frac{1}{D_i}\left(\iint\iint q_i(x)dxdxdxdx + \frac{C_{1i}}{6}x^3 + \frac{C_{2i}}{2}x^2 + C_{3i}x + C_{4i}\right), \qquad i = 1, \cdots, 4. \tag{31}$$

3.2.2. Free vibration analysis

In this section, the free vibration analysis of delaminated microbeam based on the Bernoulli-Euler beam model is studied by employing the modified couple stress theory. To this end, the differential equations of motion for the problem in hand can be obtained by applying the Hamilton's principle to the whole system as follows [35]:

$$\delta \int_{t_1}^{t_2} (T - U)dt = 0, \tag{32}$$

where t_1 and t_2 are two arbitrary time instants. Substituting Eqs. (15)-(17) and Eqs. (19)-(21) into Eq. (32) leads to the equations of motion that are presented in the subsequent sections for the constrained and free mode models.

Constrained mode

For the constrained mode model, the governing differential equations of motion for the free vibration can be derived as follows:

$$D_i \frac{\partial^4 w_i}{\partial x^4} + \rho A_i \frac{\partial^2 w_i}{\partial t^2} = 0, \qquad i = 1, 4, \tag{33}$$

$$(D_2 + D_3)\frac{\partial^4 w_2}{\partial x^4} + \rho(A_2 + A_3)\frac{\partial^2 w_2}{\partial t^2} = 0. \tag{34}$$

Using the separation of variables technique, the solution to Eqs. (33) and (34) can be written as follows:

$$w_i(x, t) = W_i(x)\cos(\omega t), \qquad (i = 1, 2, 4), \tag{35}$$

where ω and $W_i(x)$ are the natural frequency and corresponding mode shape of the ith sub-beam, respectively. Substituting Eq. (35) into Eqs. (33) and (34) and, subsequently, dividing both sides by $\cos(\omega t)$, we obtain the following fourth-order ordinary differential equation:

$$\frac{d^4 W_i(x)}{dx^4} - \lambda_i^4 W_i(x) = 0, \qquad i = 1, 4, \tag{36a}$$

$$\frac{d^4W_2(x)}{dx^4} - \lambda_2^4 W_2(x) = 0, \tag{36b}$$

where:

$$\lambda_i^4 = \frac{\rho A_i \omega^2}{D_i}, \qquad i = 1, 4,$$

$$\lambda_2^4 = \frac{\rho(A_2 + A_3)\omega^2}{D_2 + D_3}.$$

We assume a solution to the form $W_i(x) = Ce^{sx}$. Substituting the assumed solution into the differential equations (36a) and (36b), one can obtain $s = \pm\lambda$, $s = \pm\hat{i}\ \lambda$ ($\hat{I}$ is the complex variable). After some simplifications, the appropriate solution for the mode shape can be obtained as follows:

$$W_i(x) = C_i \cos(\lambda_i x) + S_i \sin(\lambda_i x) + Q_i \cosh(\lambda_i x) + R_i \sinh(\lambda_i x), \qquad i = 1, 2, 4. \tag{37}$$

It is clear that, in this case, we have 12 unknown coefficients C_i, S_i, Q_i, and R_i ($i = 1, 2$, and 4). These coefficients can be determined by 4 boundary conditions as well as 8 continuity and compatibility relations. The appropriate boundary conditions that can be applied at the support ends (i.e., $x = 0$ and $x = L$) are $W_i = 0$ and $W_i' = 0$ for the clamped condition, $W_i = 0$ and $W_i'' = 0$ for the simply supported type, $W_i'' = 0$ and $W_i''' = 0$ for the free end conditions where $i = 1$ and 4. Note that, in the aforementioned relations, the prime sign denotes differentiation with respect to x-coordinate. The continuity conditions of deflection and slope at two ends of the delamination zone are also identified as follows:

$$w_1 = w_2, \qquad w_1' = w_2', \qquad \text{at } x = L_1, \tag{38}$$

$$w_4 = w_2, \qquad w_4' = w_2', \qquad \text{at } x = L_1 + L_d. \tag{39}$$

Moreover, the compatibility conditions of shear force can be expressed:

$$D_1 w_1''' = (D_2 + D_3) w_2''', \qquad \text{at } x = L_1, \tag{40}$$

$$D_4 w_4''' = (D_2 + D_3) w_2''', \qquad \text{at } x = L_1 + L_d. \tag{41}$$

Finally, the compatibility conditions of bending moments are obtained as follows:

$$D_1 W_1'' = (D_2 + D_3) W_2'' - \frac{h_1^2}{4L_d}\left(\frac{W_1'(L_1) - W_4'(L_1 + L_d)}{\frac{1}{(\lambda+2\mu)A_2} + \frac{1}{(\lambda+2\mu)A_3}}\right), \quad \text{at } x = L_1, \tag{42}$$

$$D_4 W_4'' = (D_2 + D_3) W_2'' - \frac{h_1^2}{4L_d}\left(\frac{W_1'(L_1) - W_4'(L_1 + L_d)}{\frac{1}{(\lambda+2\mu)A_2} + \frac{1}{(\lambda+2\mu)A_3}}\right), \quad \text{at } x = L_1 + L_d, \tag{43}$$

where Eqs. (38)-(43) along with four boundary conditions provide 12 homogenous equations for 12 unknown coefficients C_i, S_i, Q_i, and R_i ($i = 1$, 2 and 4). Substituting Eq. (36) into these conditions leads to the matrix-form equations $[A]\{C_1, S_1, \cdots, Q_4, R_4\}^T = \{0\}$. To obtain a nontrivial solution to the unknown coefficients, the determinant of coefficient matrix $[A]$ must be zero, which forms the characteristic equation for the system natural frequencies. In fact, the eigenvalues and eigenvectors of the above matrix-form equations are the natural frequencies and the corresponding mode shapes of the delaminated microbeam, respectively.

Free mode

For the free mode, the equations of motion are derived as follows:

$$D_i \frac{\partial^4 w_i}{\partial x^4} + \rho A_i \frac{\partial^2 w_i}{\partial t^2} = 0, \qquad i = 1 \cdots 4. \tag{44}$$

The solution forms for the free mode model are identical to the constrained mode. Note that there are 16 unknown coefficients that can be determined by 4 boundary conditions and 12 continuity and compatibility conditions. The boundary conditions for the free mode are identical to those that are presented for the constrained mode. Moreover, the continuity conditions for deflection and slope and also compatibility conditions for the shear forces and bending moments are as follows:

The continuity conditions of the transverse deflection:

$$w_1 = w_2, \qquad w_1 = w_3, \qquad \text{at } x = L_1, \tag{45}$$

$$w_4 = w_2, \qquad w_4 = w_3, \qquad \text{at } x = L_1 + L_d. \tag{46}$$

The continuity conditions of the slope:

$$w_1' = w_2', \qquad w_1' = w_3', \qquad \text{at } x = L_1, \tag{47}$$

$$w_4' = w_2', \qquad w_4' = w_3', \qquad \text{at } x = L_1 + L_d. \tag{48}$$

The compatibility conditions of the shear forces:

$$D_1 w_1''' = D_2 w_2''' + D_3 w_3''', \qquad \text{at } x = L_1, \tag{49}$$

$$D_4 w_4''' = D_2 w_2''' + D_3 w_3''', \qquad \text{at } x = L_1 + L_d. \tag{50}$$

The compatibility conditions of the bending moments:

$$D_1 W_1'' = D_2 W_2'' + D_3 W_3'' - \frac{h_1^2}{4L_d}\left(\frac{W_1'(L_1) - W_4'(L_1 + L_d)}{\frac{1}{(\lambda+2\mu)A_2} + \frac{1}{(\lambda+2\mu)A_3}}\right), \quad \text{at } x = L_1, \tag{51}$$

$$D_4 W_4'' = D_2 W_2'' + D_3 W_3'' - \frac{h_1^2}{4L_d}\left(\frac{W_1'(L_1) - W_4'(L_1 + L_d)}{\frac{1}{(\lambda+2\mu)A_2} + \frac{1}{(\lambda+2\mu)A_3}}\right), \quad \text{at } x = L_1 + L_d. \tag{52}$$

Eqs. (45)-(52) and four appropriate boundary conditions make a set of 16 simultaneous linear homogenous algebraic equations for 16 unknown coefficients C_i, S_i, Q_i, and $R_i (i = 1 - 4)$. The frequencies and corresponding mode shapes can be obtained in a similar way that is described for the constrained mode model.

4. Numerical results

The beam model assumed here is taken to be made of epoxy with $E = 1.44$ GPa, $v = 0.38$, $\rho = 1220$ kg/m^3, and $\ell = 17.6$ μm as elastic modulus, Poisson's ratio, density, and length-scale parameter, respectively [8]. The verifications and results for the static case and free vibration case are presented in the next sections. Since incorporating the Poisson's ratio causes underestimation of deflection due to the overestimation of bending rigidity of microbeam [10,11], the Poisson's ratio is assumed here to be zero. For all considered examples, unless mentioned otherwise, the beam's dimensions are $L = 20h_1$ and $b = 2h_1$. Different delamination parameters vary, and their effects on the microbeam behavior are investigated.

4.1. Static analysis

As shown in Figure 3, a cantilever beam with central delamination, which is subjected to a vertical force at the free end, is considered here. The central delamination refers to a delamination whose center coincides with the beam center. In order to verify the present formulations, the delamination length is considered infinitesimally small (i.e., $L_d = 0.01L$), and the constrained mode model is applied. For all numerical examples in the static analysis, the load magnitude is taken to be $P = 100$ μN [8].

The deflection of the microbeam based on the present formulation is depicted in Figure 4. We can observe that the deflection of the delaminated microbeam with extremely small delamination length is identical to the result reported previously by Park et al. [8] for an intact microbeam with the same conditions.

The effect of delamination length on the deflection of the microbeam is investigated in Figure 5. In this case, the central delamination is placed on the mid plane of the beam (i.e., $h_2 = h_3$). It is worth mentioning that, in this figure and also in Figures 6-8, the blue lines in the left and right sides of the delamination region refer to the deflection of sub-beams 2 and 3, respectively. It is obvious that the beam's deflection directly depends on the delamination length so that it increases when the delamination length

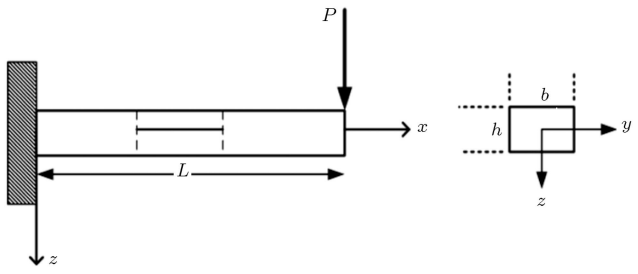

Figure 3. The cantilever beam with the central delamination subjected to a point load P at its free end.

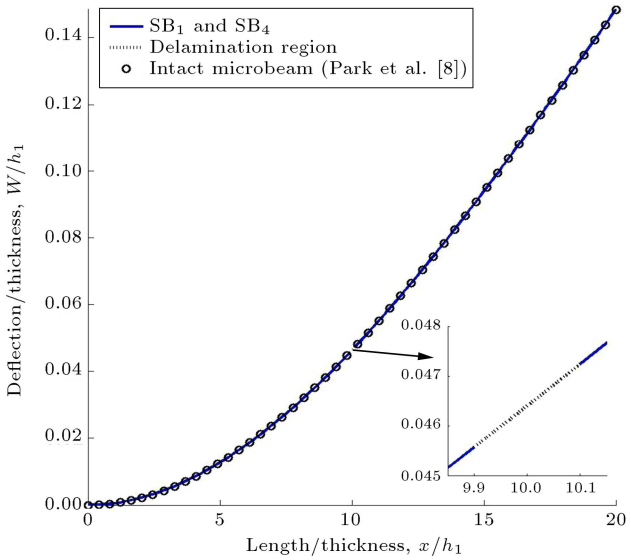

Figure 4. Static bending deflection for the cantilever microbeam subjected to a point load at its free end (see Figure 3 with $P = 100$ μN). In order to verify our model, the delamination length is considered very small (i.e., $L_d = 0.01L$) and the beam deflection is compared with the static deformation of intact microbeam obtained in [8]. Note that SB$_i$ is abbreviated for ith sub-beam ($i = 1, 4$), and the delamination region is referred to sub-beams 2 and 3.

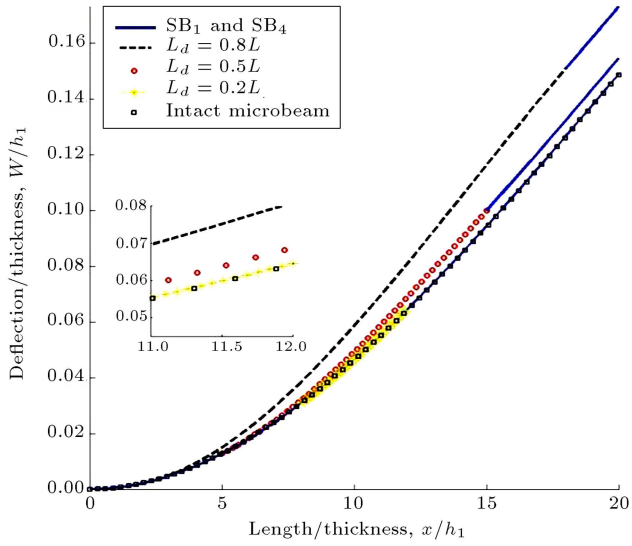

Figure 5. Effect of delamination length on the deflection of cantilever micro beam (see Figure 3) with $h_2 = h_3$ and $P = 100$ μN. Note that the solid blue line refers to the deflection of the sub-beams 1 and 4, before and after the delamination zone.

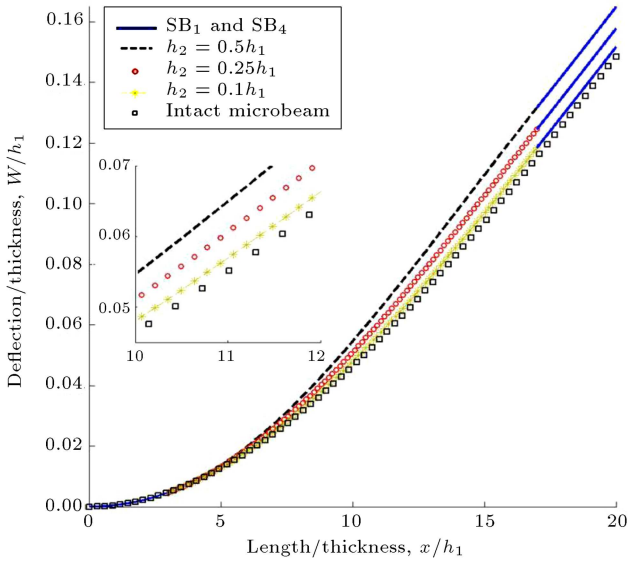

Figure 6. Effect of delamination thicknesswise location on the deflection of cantilever microbeam (see Figure 3) with $L_d = 0.7L$ and $P = 100$ μN. Note that the solid blue line refers to the deflection of sub-beams 1 and 4, before and after the delamination zone.

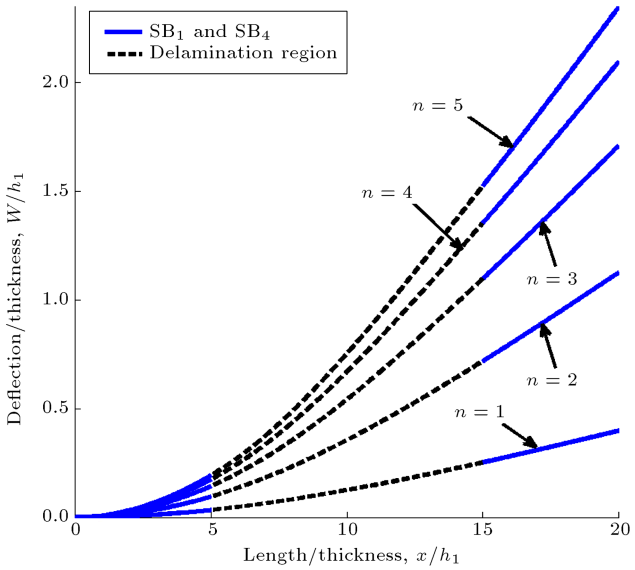

Figure 7. Effect of length-scale parameter on the deflection of cantilever microbeam (see Figure 3) with $h_2 = h_3 = 0.5h_1$, $L_d = 0.5L$, $P = 100$ μN, $h_1 = 20$ μm and $n = h_1/\ell$. Note that the solid blue line refers to the deflection of the sub-beams 1 and 4, before and after the delamination zone.

increases. This occurrence is because the delamination decreases the beam's overall stiffness.

Figure 6 illustrates the effect of thicknesswise location of the delamination on the static deflection of the delaminated microbeam. In this case, the length of the central delamination is considered to be $L_d = 0.7L$, and three different thicknesswise locations are considered. Therefore, it is observed that as the

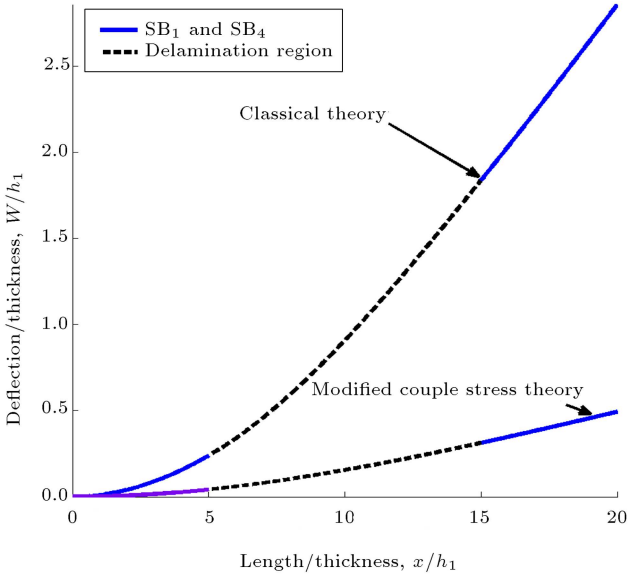

Figure 8. Effect of length-scale parameter on the deflection of the cantilever microbeam (see Figure 3) with $h_2 = h_3 = 0.5h_1$, $L_d = 0.5L$ and $P = 100$ μN. Note that the solid blue line refers to the deflection of sub-beams 1 and 4, before and after the delamination zone.

delamination gets closer to the mid-plane of the beam, the corresponding deflection of the beam is higher.

The effect of length-scale parameter on the deflection of the delaminated microbeam is depicted in Figure 7. For this example and the next one, a central delamination ($h_2 = h_3 = 0.5h_1$) is considered, and its length is considered to be $L_d = 0.5L$. It is found that as the value of the length-scale parameter ($\ell = h_1/n$) increases, the static deflection of the delaminated microbeam decreases due to the stiffening effect of the couple stress theory.

As the final example of static section, the deflections predicted by the modified couple stress theory and the classical theory are compared in Figure 8. Also, it is worth mentioning that by letting $\ell = 0$, the expressions for the classical Bernoulli-Euler beam theory can be achieved from the expressions obtained in this study. From Figure 8, it is clear that the beam modeled on the basis of the modified couple stress theory is stiffer than those predicted by the classical beam theory.

4.2. Free vibration analysis

Effects of delamination parameters on the free vibration characteristics of the microbeam are investigated in this section. In this study, applied three types of boundary conditions are as follows: Clamped-Free (CF), Simple-Simple (SS), and Clamped-Simple (CS). Similar to the static bending case, the Poisson's effect is not included in calculating the numerical results. It is obvious that by letting delamination length be very small, the results of the delaminated microbeam tend to the intact one. This can be used in order to

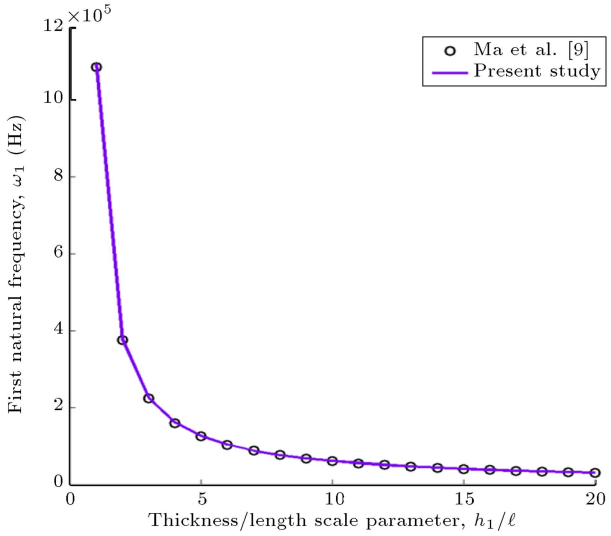

Figure 9. Fundamental natural frequency of the simply supported intact microbeam.

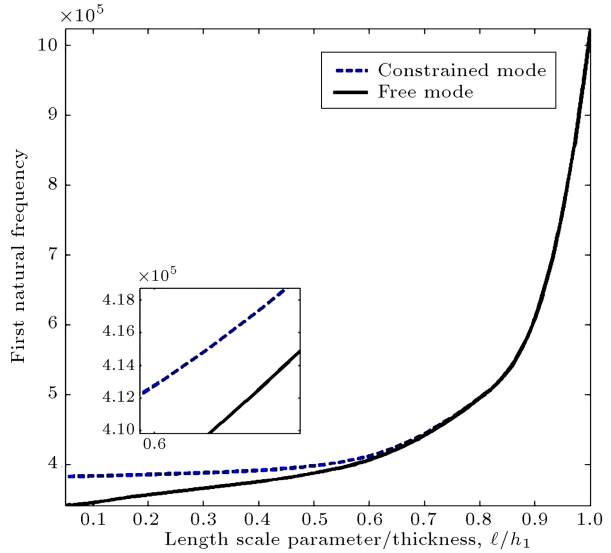

Figure 10. The effect of length-scale parameter on the fundamental natural frequency (in HZ) of the delaminated simply supported microbeam with $h_2 = h_3 = 0.5h_1$, $L_d = 0.5L$, $h_1 = 20$ μm, and $L_1 = L_4$.

verify the present vibration analysis of the delaminated microbeam.

In order to verify present formulations, a microbeam with SS boundary conditions is considered [9]. The fundamental natural frequency of this microbeam is compared with that reported by Ma et al. [9] and depicted in Figure 9. We can clearly observe excellent agreement between the present results and those obtained by Ma et al. [9].

The effect of length-scale parameter on the dynamic characteristics of the delaminated microbeam based on the free and constrained mode models is presented in Figure 10. In order to obtain this figure, the value of ℓ is varied and the beam's thickness is kept constant (i.e., $h_1 = 20$ μm). It is obvious from the figure that the frequencies obtained by the free mode model are smaller than those derived by the constrained mode model are. In other words and as discussed in [27-30] for classical delaminated beams, the free and constrained mode models can be considered as the lower and upper bounds of the natural frequencies, respectively (neglecting the nonliner effects due to the contact interaction between the two surfaces of delamination). Likewise, by decreasing the material length-scale parameter, the fundamental natural frequency decreases. In addition, the difference between the natural frequencies predicted by free and constrained mode models increases by decreasing the material length-scale parameter. This indicates that the role of opening phenomenon in the mode shapes of the free model is more distinct in the lower values of material length-scale parameter.

The effects of delamination length and its thicknesswise location on the first natural frequency of the microbeam with central delamination are presented in Figure 11 for three different boundary conditions. The results of these figures are obtained based on the constrained model. It is observed that by increasing the delamination length, the fundamental natural frequency of the delaminated microbeam decreases. As stated before, this is due to the reduction in beam's overall stiffness. Moreover, it should be mentioned that as the delamination length becomes larger, the rate of the frequency changes becomes higher. In addition, the effect of thicknesswise location of delamination is clearly shown in these figures. Results show that the microbeams with the mid-plane delamination have the lower natural frequencies compared to the microbeams with the delamination closer to the free surfaces.

The effects of spanwise location of delamination on the first natural frequencies of microbeam are illustrated in Figure 12. The results are obtained based on the constrained mode model for three different thicknesswise locations of $h_2/h_1 = 0.1$, 0.2, and 0.5. In this case, a constant delamination length $L_d = 0.4L$ is considered. It is deduced that the presence of delamination in the vicinity of the restricted supports (e.g., clamped or hinged) leads to the reduction of the overall system stiffness; consequently, the fundamental frequency of the microbeam reduces too. In other words, when the delamination is shifted towards either of the restricted supports, the natural frequencies would decrease accordingly. Moreover, by referring to Figure 12(b), the maximum natural frequency for the beam with SS end conditions occurs when the delamination is placed at the middle of the beam. However, for the beams with CF (Figure 12(a)) and CS (Figure 12(c)) boundary conditions, the maximum points can be found when the delamination is close to the free end and simple end of the beam, respectively.

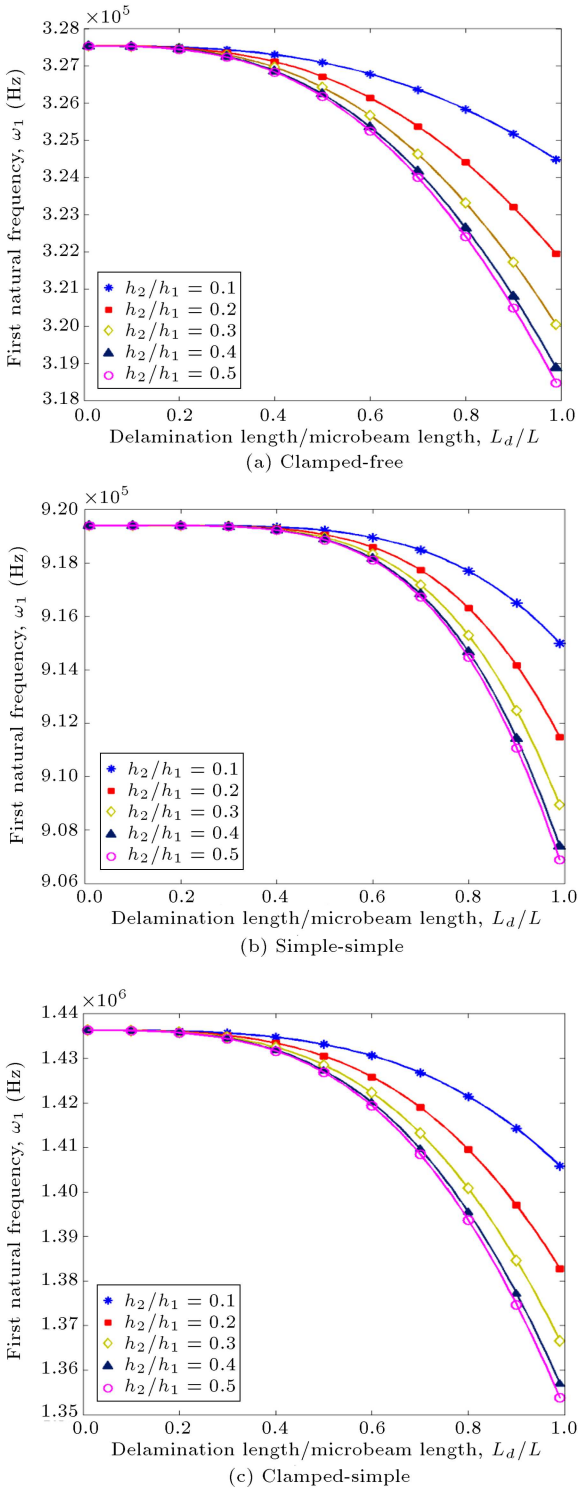

Figure 11. Fundamental frequencies versus dimensionless delamination length for different thicknesswise locations of delamination in microbeams with $h_1 = 20$ μm and $L_1 = L_4$.

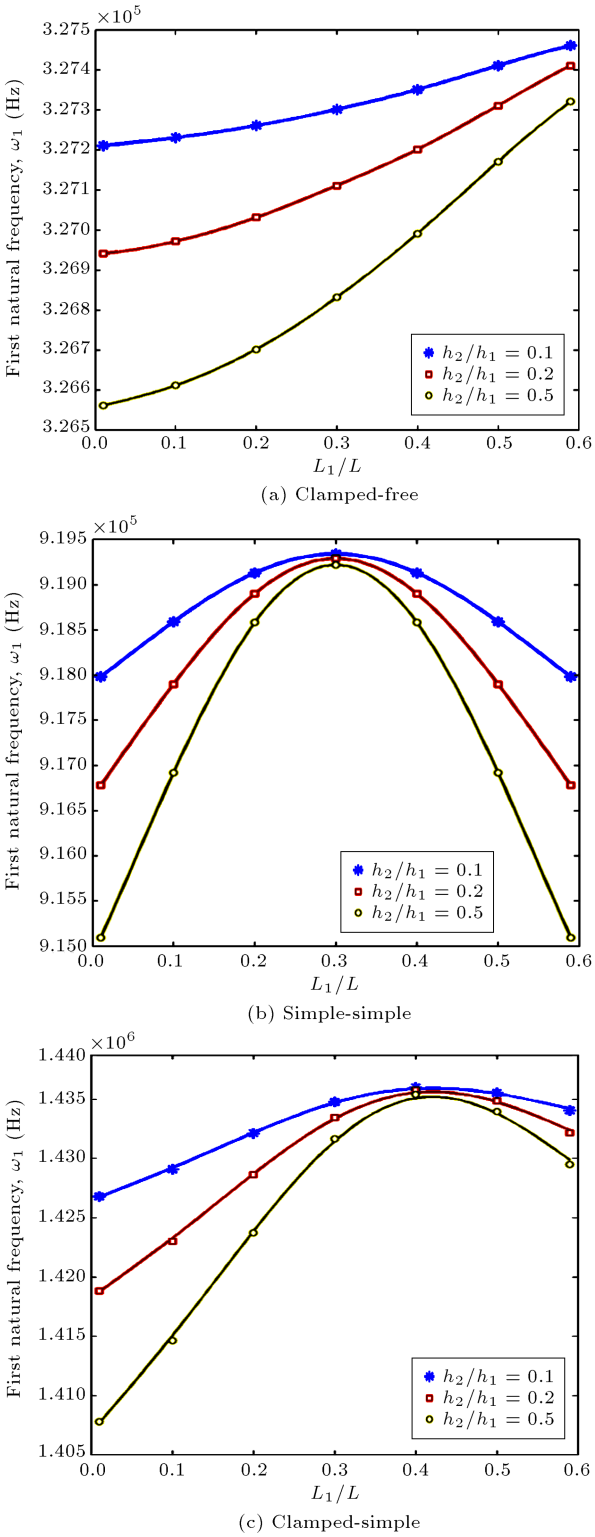

Figure 12. Fundamental frequencies versus spanwise location of the delamination for the microbeam with $L_d = 0.4L$, $h_1 = 20$ μm, $L_1 = L_4$ and three different thicknesswise locations h_2/h_1.

The fundamental natural frequencies of simply supported beams with a central delamination are presented in Figure 13 based on the free and constrained mode models. The results have been obtained with respect to two different thicknesswise locations of $h_2/h_1 = 0.1$ and 0.4. We can observe that the lower and upper bounds of the natural frequencies are obtained

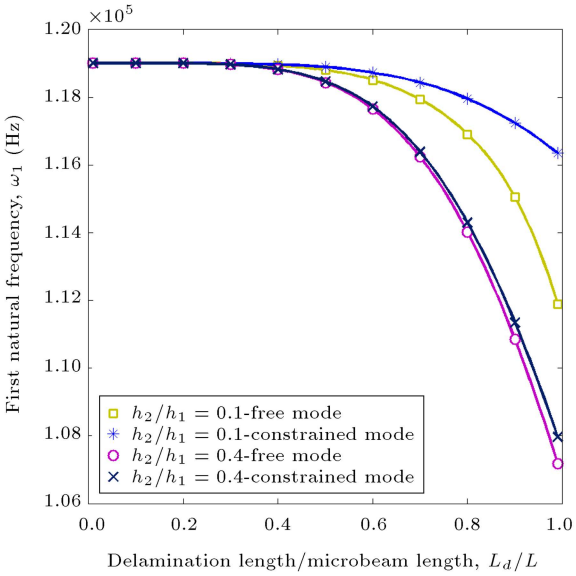

Figure 13. Fundamental natural frequencies based on the free and constrained mode theories for a simply supported microbeam with $h_1 = 75$ μm, and $L_1 = L_4$.

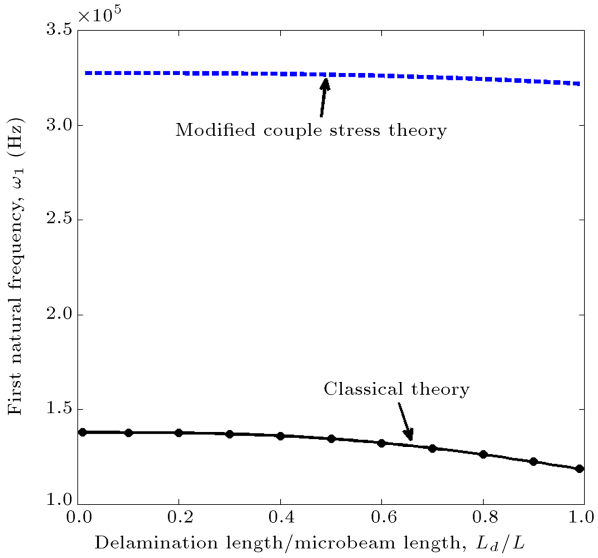

Figure 14. First natural frequency versus dimensionless delamination length for a cantilever microbeam based on the modified couple stress and classical theories ($h_1 = 20$ μm, $L_1 = L_4$, $h_2/h_1 = 0.2$, and the constrained mode model is used).

using the eigenvalue solutions for the 'free' and 'constrained' modes of the delaminated layers, respectively. If the delamination is located close to the beam mid-plane, the natural frequencies of the beam obtained by the free and constrained modes are almost the same. This is due to the fact that no "opening mode" is observed for this case. However, when the delamination is located close to the free surface of the beam, the role of so-called "opening modes" is distinctive. This can be explained by the fact that the stiffnesses of the second and third sub-beams are close when the delamination is placed at $h_2/h_1 = 0.4$. On the other hand, when the delamination is placed at thicknesswise location $h_2/h_1 = 0.1$, the difference between the stiffnesses of sub-beams 2 and 3 is relatively high.

In order to compare the results predicted by the modified couple stress theory with those obtained from the classical theory, the fundamental natural frequencies of a cantilever microbeam versus the dimensionless delamination length are depicted in Figure 14. For this purpose, the thickness of $h_1 = 20$ μm and delamination's thicknesswise location of $h_2/h_1 = 0.2$ are considered. The results are calculated based on the constrained mode model. It is obvious from the figure that the frequencies obtained by classical beam theory are less than half of those predicted by the modified couple stress theory. This can clearly demonstrate that the results obtained according to the classical theory are not accurate enough for the present system, since the role of length-scale parameter is not incorporated.

The first mode shapes of a microbeam with clamped-clamped boundary conditions and based on the free mode models are depicted in Figure 15. The single delamination with two different delamination lengths is positioned at two different thicknesswise locations. From these diagrams, one can observe that the first mode shape of the beam does not show any opening behavior when the delamination is located near the mid-plane (see Figure 15(a) and (b)) and also when the short delamination is placed near the free surface (see Figure 15(c)). However, once the longer delamination is located near the free surface (see Figure 15(d)), we can clearly see the opening mode phenomenon in the delamination region. Therefore, the delamination length and its thicknesswise location have significant effects on the occurrence of opening mode phenomenon for the fundamental mode.

Finally, the effects of delamination spanwise location on the mode shape of a clamped-clamped microbeam are illustrated in Figure 16. It is clearly demonstrated that when the delamination spanwise location is not central, the normal mode shape loses its symmetry and becomes asymmetric.

5. Conclusions

An analytical solution for the static and dynamic analyses of the delaminated microbeams based on the modified couple stress theory was presented in this work. We evaluated the effects of delamination geometry and locations on the static and dynamic responses of the delaminated non-classical size-dependent beam-like components. Since this study is the first to deal with the delaminated microbeams, we believe that the results presented in this study can be used as a benchmark for similar works in the future. Based on

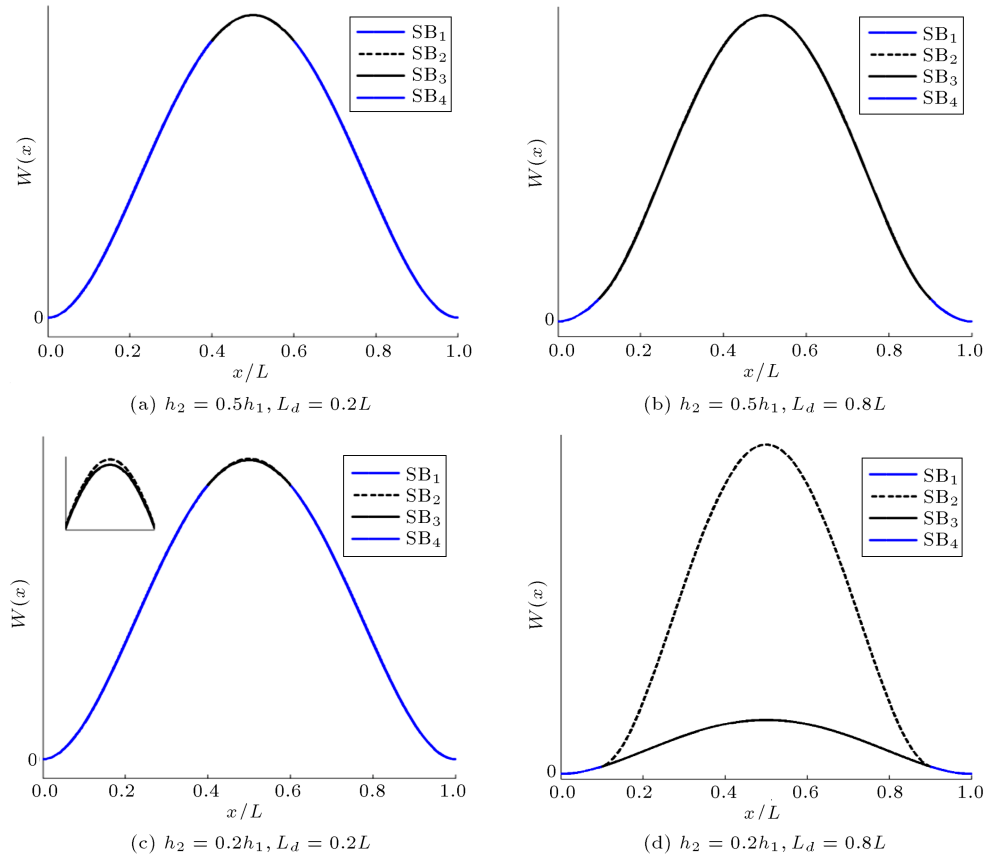

(a) $h_2 = 0.5h_1, L_d = 0.2L$ (b) $h_2 = 0.5h_1, L_d = 0.8L$

(c) $h_2 = 0.2h_1, L_d = 0.2L$ (d) $h_2 = 0.2h_1, L_d = 0.8L$

Figure 15. First normal mode shape of the delaminated clamped-clamped microbeam with different delamination lengths and thicknesswise locations ($L_1 = L_4$ and the free mode model are used).

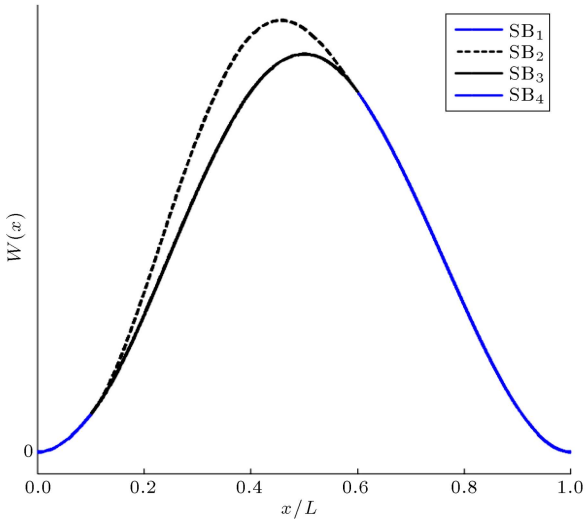

Figure 16. First mode shape of the delaminated microbeam ($h_2 = 0.2h_1$, $L_d = 0.5L$, $L_1 = 0.1L$, and the free mode model are used).

the obtained results, the following observations have been made:

1. It is found that the static and dynamic responses of microbeam are sensitive to the delamination parameters. The existence of such a delamination can increase the microbeam's deflection in static and dynamic cases;
2. For the delaminated microbeam, when the delamination shifts towards the mid-plane of beam cross-section, higher static transverse deformation has been observed for the beam;
3. Once the delamination length is more than half of the beam's length, significant changes will be obtained in the microbeam's natural frequencies. In other words, as the delamination length increases, the natural frequencies decrease;
4. By moving the delamination closer to the mid-plane of beam cross-section, the natural frequencies decrease further;
5. The fundamental frequency decreases as the delamination shifts towards the restricted supports;
6. The difference between the natural frequencies obtained from the free and constrained mode models can indicate that the presence of opening mode phenomenon between the delaminated layers can significantly change the microbeam's free vibration characteristics;
7. It has been observed that the natural frequencies of microbeam decrease as the material length-scale

parameter decreases. In addition, the difference between the frequencies obtained from the free and constrained mode models increases when the value of length-scale parameter decreases.

References

1. Hung, E.S. and Senturia, S.D. "Extending the travel range of analog-tuned electrostatic actuators", *J. Microelectromech. S.*, **8**(4), pp. 497-505 (1999).
2. Pei, J., Tian, F., and Thundat, T. "Novel glucose biosensor based on the microcantilever", *Anal. Chem.*, **76**, pp. 292-297 (2004).
3. Pereira, R.D.S. "Atomic force microscopy as a novel pharmacological tool", *Biochem. Pharmacol.*, **62**, pp. 975-983 (2001).
4. Jafari-Talookolaei, R.A., Abedi, M., Şimşek, M., and Attar, M. "Dynamics of a micro scale Timoshenko beam subjected to a moving micro particle based on the modified couple stress theory", *J. Vib. Control*, **24**(3), pp. 527-548 (2018).
5. Mindlin, R. and Tiersten, H. "Effects of couple-stresses in linear elasticity", *Arch. Ration. Mech. An.*, **11**, pp. 415-448 (1962).
6. Toupin, R.A. "Elastic materials with couple-stresses", *Arch. Ration. Mech. An.*, **11**, pp. 385-414 (1962).
7. Yang, F., Chong, A., Lam, D., and Tong, P. "Couple stress based strain gradient theory for elasticity", *Int. J. Solids Struct.*, **39**, pp. 2731-2743 (2002).
8. Park, S.K. and Gao, X.L. "Bernoulli-Euler beam model based on a modified couple stress theory", *J. Micromech. Microeng.*, **16**, pp. 2355-2359 (2006).
9. Ma, H.M., Gao, X.L., and Reddy, J. "A microstructure-dependent Timoshenko beam model based on a modified couple stress theory", *J. Mech. Phys. Solids*, **56**, pp. 3379-3391 (2008).
10. Dehrouyeh-Semnani, A.M. and Nikkhah-Bahrami, M. "A discussion on incorporating the Poisson effect in micro-beam models based on modified couple stress theory", *Int. J. Eng. Sci.*, **86**, pp. 20-25 (2015).
11. Reddy, J.N. and El-Borgi, S. "Eringen's nonlocal theories of beams accounting for moderate rotations", *Int. J. Eng. Sci.*, **82**, pp. 159-177 (2014).
12. Kahrobaiyan, M.H., Asghari, M., Rahaeifard, M., and Ahmadian, M.T. "Investigation of the size-dependent dynamic characteristics of atomic force microscope microcantilevers based on the modified couple stress theory", *Int. J. Eng. Sci.*, **48**, pp. 1985-1994 (2010).
13. Asghari, M., Kahrobaiyan, M.H., and Ahmadian, M.T. "A nonlinear Timoshenko beam formulation based on the modified couple stress theory", *Int. J. Eng. Sci.*, **48**, pp. 1749-1761 (2010).
14. Akgöz, B. and Civalek, Ö. "Strain gradient elasticity and modified couple stress models for buckling analysis of axially loaded micro-scaled beams", *Int. J. Eng. Sci.*, **49**, pp. 1268-1280 (2011).
15. Simsek, M. and Reddy, J.N. "Bending and vibration of functionally graded micro-beams using a new higher order beam theory and the modified couple stress theory", *Int. J. Eng. Sci.*, **64**, pp. 37-53 (2013).
16. Akgöz, B. and Civalek, Ö. "Free vibration analysis of axially functionally graded tapered Bernoulli-Euler micro-beams based on the modified couple stress theory", *Compos. Struct.*, **98**, pp. 314-322 (2013).
17. Mohammad Abadi, M. and Daneshmehr, A.R. "An investigation of modified couple stress theory in buckling analysis of micro composite laminated Euler-Bernoulli and Timoshenko beams", *Int. J. Eng. Sci.*, **75**, pp. 40-53 (2014).
18. Darijani, H. and Mohammadabadi, H. "A new deformation beam theory for static and dynamic analysis of micro-beams", *Int. J. Mech. Sci.*, **89**, pp. 31-39 (2014).
19. Dai, H.L., Wang, Y.K., and Wang, L. "Nonlinear dynamics of cantilevered micro-beams based on modified couple stress theory", *Int. J. Eng. Sci.*, **94**, pp. 103-112 (2015).
20. Mohammad-Abadi, M. and Daneshmehr, A.R. "Size dependent buckling analysis of micro-beams based on modified couple stress theory with high order theories and general boundary conditions", *Int. J. Eng. Sci.*, **74**, pp. 1-14 (2014).
21. Simsek, M. "Nonlinear static and free vibration analysis of micro-beams based on the nonlinear elastic foundation using modified couple stress theory and He's variational method", *Compos. Struct.*, **112**, pp. 264-272 (2014).
22. Ghayesh, M.H., Farokhi, H., and Amabili, M. "Nonlinear dynamics of a microscale beam based on the modified couple stress theory", *Compos. Eng.*, **50**, pp. 318-324 (2013).
23. Farokhi, H., Ghayesh, M.H., and Amabili, M. "Nonlinear dynamics of a geometrically imperfect micro-beam based on the modified couple stress theory", *Int. J. Eng. Sci.*, **68**, pp. 11-23 (2013).
24. Wang, J.T.S., Liu, Y.Y., and Gibby, J.A. "Vibrations of split beams", *J. Sound Vib.*, **84**, pp. 491-502 (1982).
25. Mujumdar, P.M. and Suryanarayan, S. "Flexural vibrations of beams with delaminations", *J. Sound Vib.*, **125**, pp. 441-461 (1988).
26. Shen, M.H. and Grady, J.E. "Free vibrations of delaminated beams", *AIAA J.*, **30**, pp. 1361-1370 (1992).
27. Della, C.N., Shu, D., and MSRao, P. "Vibrations of beams with two overlapping delaminations", *Compos. Struct.*, **66**, pp. 101-108 (2004).
28. Manoach, E., Warminski Mitura, J.A., and Samborski, S. "Dynamics of a composite Timoshenko beam with delamination", *Mech. Res. Commun.*, **46**, pp. 47-53 (2012).
29. Kargarnovin, M.H., Ahmadian, M.T., and Jafari-Talookolaei, R.A. "Forced vibration of delaminated Timoshenko beams subjected to a moving load", *Sci. Eng. Compos. Mater.*, **19**, pp. 145-157 (2012).

30. Kargarnovin, M.H., Jafari-Talookolaei, R.A., and Ahmadian, M.T. "Vibration analysis of delaminated Timoshenko beams under the motion of a constant amplitude point force traveling with uniform velocity", *Int. J. Mech. Sci.*, **70**, pp. 39-49 (2013).

31. Szekrényes, A. "Coupled flexural-longitudinal vibration of delaminated composite beams with local stability analysis", *J. Sound Vib.*, **333**, pp. 5141-5164 (2014).

32. Szekrenyes, A. "A special case of parametrically excited systems: Free vibration of delaminated composite beams", *Eur. J. Mech. A-Solid*, **49**, pp. 82-105 (2015).

33. Attar, M., Karrech, A., and Regenauer-Lieb, K. "Nonlinear modal analysis of structural components subjected to unilateral constraints", *J. Sound Vib.*, **389**, pp. 380-410 (2016).

34. Attar, M., Karrech, A., and Regenauer-Lieb, K. "Nonlinear analysis of beam-like structures on unilateral foundations: a lattice spring model", *Int. J. Solids Struct.*, **88**, pp. 192-214 (2016).

35. Clive, L.D. and Shames, I.H., *Solid Mechanics, A Variational Approach*, Springer (2013).

Biographies

Ramazan-Ali Jafari-Talookolaei is currently an Assistant Professor at the School of Mechanical Engineering, Babol Noshirvani University of Technology. He obtained his BSc in Mechanical Engineering from Shahrood University of Technology in 2002, his MSc and PhD degrees in Mechanical Engineering from Sharif University of Technology in 2004 and 2013, respectively. His current research interests include laminated composite structures, micro and nano structures, finite-element method, analytical solutions, dynamics, vibration, linear and non-linear analyses, and damaged structures. He has published 3 books and more than 60 journal and conference papers.

Nima Ebrahimzade is currently a PhD candidate of Mechanical Engineering at the School of Mechanical and Systems Engineering, Newcastle University-UK. He received his MSc in Mechanical Engineering from Babol Noshirvani University of Technology-Iran in 2016. His Research interests include nonlinear dynamics and vibration, aeroelasticity, and MEMS.

Saeed Rashidi-Juybari received his MSc degree in Mechanical Engineering from the Department of Mechanical engineering at Babol Noshirvani University of Technology, Iran in 2016 and his BSc degree from the University of Tafresh, Iran. His research interests are fluid-structure interaction, offshore and ocean engineering, wave energy conversion, and structural vibration.

Khashayar Teimoori is a PhD candidate of Mechanical Engineering and Adjunct Lecturer in the Grove School of Engineering at the City College of the City University of New York, where he obtained his MSc degree in Mechanical Engineering. He completed his BSc in Mechanical Engineering at Tehran Science and Research Branch of the Islamic Azad University under the supervision of late distinguished Professor Mohammad H. Kargarnovin. His research interests include both pure and applied scientific topics in Mechanical Engineering and Mathematical Sciences such as; mechanical vibration, applied mechanics in fluid-structure/solid interactions, electro-mechanobiological systems, however, the interests are not limited to the mentioned topics.